IEEE Access
Multidisciplinary ⋮ Rapid Review ⋮ Open Access Journal

Received 21 February 2022, accepted 21 April 2022, date of publication 25 April 2022, date of current version 11 July 2022.

Digital Object Identifier 10.1109/ACCESS.2022.3170410

IQ Symbols Processing Schemes With LSTMs in OFDM System

JUN LI[1], TONGLIANG XIN[1], BO HE[2], AND WENXIN LI[1]
[1]School of Information and Automation, Qilu University of Technology (Shandong Academy of Sciences), Jinan 250353, China
[2]School of Information Science and Engineering, Shandong University, Qingdao 266237, China

Corresponding author: Jun Li (rogerjunli@sdu.edu.cn)

This work was supported in part by the National Natural Science Foundation of China (NSFC) under Grant 12005108; and in part by the Shandong Provincial Natural Science Foundation, China, under Grant ZR2020QF016.

ABSTRACT IQ modulation enjoys great popularity in wireless communication. Its main advantage is the symmetric convenience of combining independent signal components into a single composite signals in the transmitter. And it splits the composite signal into its independent components in the receiver. However, due to the limitations of communication facilities and imperfect channel environments, the symbols will be distorted. In this paper, we propose several signal processing schemes based on deep learning (DL) neural networks (i.e., long short-term memory (LSTM)) to process signal in an end-to-end manner, known as DLA, EDLA and PDNet. These schemes combine with advanced DL architectures and data-driven models for complex-valued signal processing. Enlightened by IQ demodulation ideas, we adopt LSTMs to develop several schemes to implement different functions (i.e., signal detection and peak to average power ratio (PAPR) reduction). The simulation results show that the schemes have significant performance improvement in bit error rate (BER) while reducing the probability of high PAPR.

INDEX TERMS IQ modulation, deep learning, ensemble networks, OFDM system.

I. INTRODUCTION

What is IQ modulation? It is widely used in wireless communication systems for its high-speed data transmission rate and manageable implementations [1]. Different from traditional analog modulation, like AM, DSB, and FM, digital modulation adopts novel the IQ modulation structure to modulate initial 0/1 bitstreams. In general, digital modulation maps the raw bitstreams to the IQ coordinate system in a certain way. The modulated symbols can be represented by the sum of two orthogonal branches that come from I-channel and Q-channel, respectively.

Orthogonal frequency division multiplexing (OFDM) is a remarkable and popular multi-carrier transmission scheme [2]. The equalization of OFDM system is the critical point of its practice. And it is mainly to eliminate or reduce the inter-symbol interference caused by multipath time delay. It contains linear and nonlinear methods.

Machine learning (ML) is a branch of artificial intelligence (AI) and has developed various algorithms after many years (e.g., support vector machine (SVM) and neural network (NN)) [3]. DL is a splendid algorithm and derived initially from the biological neural system schemes. For the DNN, the weighted sum of several inputs with bias is fed into an activation function $\sigma(\cdot)$ (i.e., sigmoid, ReLU) to obtain the outputs y, which is defined as the forward propagation architecture. In the backpropagation process, the parameters (i.e., weights, bias) are optimized after several epochs for the expected outputs. We can enhance the computation performance by adding more neurons and hidden layers.

It is demonstrated that DL can be applied to tackle many wireless communication problems (i.e., modulation recognition, channel decoding, detection) [3]. Modulation recognition distinguishes modulation schemes from the received noisy signal and contains several procedures (e.g., processing, feature extraction, classification). The modulation methods vary with the changes of distance and surrounding environments. Studies were conducted for many years and mainly divided into two categories (i.e., decision theoretic, pattern recognition) [4]. The novel architecture proposed in [4] has a powerful performance in distinguishing noise-corrupted signal modulation method from 13 types of modulated signals. It can be regarded as an ensemble network and includes a four-layer network and two two-layer networks. The input of the four-layer network contains the amplitude, phase and frequency information of the signal, which are obtained from traditional feature extraction techniques. Due to the difficulties of disguising the similar

The associate editor coordinating the review of this manuscript and approving it for publication was Zihuai Lin.

modulation methods (i.e., MASK, MFSK), the two two-layer networks were proposed to refine ASK2, ASK4, FSK2 and FSK4.

In the scheme proposed in [5], the input and output of the networks are vectors of size N which presents N-dimensional log-likelihood ratios (LLRs) received from channels and N-bits decoded codewords, respectively. However, the new requirements of 5G and other communication systems (e.g., massive MIMO, mmWave) enhance its computational complexity. In [6], a novel signal detection scheme based on an adaptive ensemble DL algorithm in SC-FDE systems was proposed, and it adopted LSTMs to detect signals. In that paper, the authors described the designs based on the SC-FDE system combining DL algorithm and adaptive ensemble algorithm. It demonstrates that LSTMs can achieve better performance and reliability than the traditional schemes. Thereby, the DL methods show a stable performance and the ability to further improve conventional communication systems.

[7] proposed a signal processing scheme based on fully connected DNN in OFDM system, and it exploited DL to process OFDM symbols in an end-to-end manner. The proposed DL approach estimated CSI implicitly and recovered the transmitted symbols directly. However, a massive amount of labeled data is needed for network training, and the data-driven model will reach its performance limitation, which will be illustrated in part A of Section III.

Recently, the authors in [8] considered channel coefficients with noise as the mumbling in the field of natural language processing (NLP). This is a novel idea that migrates the well-established NLP ideas into communication signal processing. It first constructs an embedding layer network, which can be regarded as a mapping network, avoiding the computational complexity caused by complex numbers. Then it proposed a channel predictor for block seq2seq model, which can predict the posterior moments based on the channel coefficients of the previous moments, and it also verifies the feasibility of the design through indoor and outdoor tests. Its signal processing idea is completely different from this paper, but at the same time, it provides new ideas for signal processing methods. The authors of the reference [9] considered the channel estimation under a massive MIMO system and used a data-driven model for signal processing, and the simulation results verified the feasibility of the design. However, for the data-driven model, the results are reliable but untrustworthy, which is due to the fact that we treat the signal processing procedures as a black box in which the parameters are not interpretable. The reference [10], on the other hand, verified the feasibility of using deep convolutional networks for channel estimation of sparse channels. And it was compared with compressed sensing techniques with a 2% performance improvement. In [11], a model-driven based channel estimation and feedback design for millimeter-wave massive MIMO was proposed, which has superior performance for signal processing of complex communication systems. Recent studies have shown the advantages of the DL approaches in communication fields.

The motivation of this paper is mainly to explore the feasibility and validation of deep learning networks applied to traditional communication architectures. For the widely used IQ structure, the LSTMs are used to realize signal detection during digital baseband signal processing at the demodulation site, eliminating or reducing inter-symbol interference caused by multipath and channel gain, and restoring the original signal. The main contributions of the article are as follows.

- We utilize thousands of trainable parameters for signal processing instead of existing signal detection and recovery algorithms. Although most neural networks do not support complex number operations, we still design the network for imitation. These parameters represent the filtering variables, and matrix operations can be implemented to obtain the expected output.
- We propose three different schemes, all of which are based on LSTM networks. It has a large number of parameters, and is especially good at processing sequence data and has superior fitting capabilities.
- This paper can be divided into two parts, one is for baseband signal processing in OFDM systems, and the other is for PAPR reduction based on deep learning solutions.
- To verify the feasibility under different indicators, we test the robustness and feasibility of the model through simulations and existing classic algorithms and peer designs. The simulation results demonstrate that, by utilizing neural networks as an alternative for processing large number of computational problems involved in communication, the computational complexity and accuracy are significantly improved compared to traditional algorithms.

Notations: In this paper, scalar variables are presented as normal-face letters. Vectors and matrix denote as boldface lower and upper-case letters, respectively. $\|\mathbf{A}\|_F$ is the Frobenius norm of matrix $\mathbf{A}$. And $\left(\hat{B}\right)$ represents the estimation of B.

The remainder of this paper is organized as follows. Section II describes the structure of the OFDM system with IQ modulation and the algorithms related to signal decoding. Section III introduces the designs based on LSTM neural networks, and the performance of BER and PAPR reduction based on the proposed scheme will be simulated and discussed in this section. Finally, Section IV concludes this paper.

II. OFDM SYSTEM MODEL WITH IQ MODULATION AND LSTM

In this section, it contains two sub-sections that elaborate the expert knowledge of IQ modulation and LSTM. In the description of the formula and the structure diagram, the details are explained clearly, paving the way for the next step to combine them. It focuses on describing the combinable points and verifies the feasibility of the designs in this article.

A. OFDM SYSTEM MODEL WITH IQ MODULATION

The OFDM system with IQ modulation/demodulation model is shown in FIGURE 1. Firstly, it is the equal-probability unipolar non-return-to-zero codes for simulation and channel coding, such as adding parity check codes to increase the signal reception accuracy. And we convert the digital signals into analog ones through a digital to analog converter (DAC), and transform the source codes through serial to parallel to obtain parallel data. Then it is divided into two branches (i.e., I and Q channel) which process the data separately. Finally, we transmit the modulated analog signal through a radio frequency (RF) facility. The working principles of the receiver are in reverse. Assuming that signal travel the fast fading and additive white Gaussian noise (AWGN) channels, the received signal can express as

$$r(n) = s(n) * g(n) + \tilde{N}(n) \tag{1}$$

where $s(n)$ denotes the transmitted OFDM symbols, and $g(n)$ denotes the CSI. Also, $\tilde{N}(n)$ denotes the AWGN, and $*$ denotes the linear convolution operation of discrete sequences.

Assuming that the baseband signal $s(t)$ is a cosine signal with low-frequency (e.g.,10KHZ), modulation is that signal multiplies a cosine signal with a high frequency to obtain the transmitted radio frequency signal $A\cos(wt)\cdot\cos(w_c t)$, where A denotes the amplitude of the signal and is a real number, and w represents the frequency of the baseband signal, and $\cos(w_c t)$ denotes the carrier with high frequency.

The radio frequency signal is transmitted and received by the transmitting and receiving antennas. In the demodulator, a carrier signal $\cos(w_c t)$ is again multiplied by the received signal to obtain

$$s_{\mathrm{Re}}(t) = \frac{A}{2}\cdot\cos(wt) + \frac{A}{2}\cdot\cos(wt)\cos(2w_c t) \tag{2}$$

where $s_{\mathrm{Re}}(t)$ includes the low-frequency signal $\cos(wt)$ and a high-frequency component $\cos(wt)\cos(2w_c t)$, and a low-pass filter is used to filter out the high-frequency component, and the transmitted baseband signal can be obtained.

The IQ demodulation scheme in the receiver is shown in FIGURE 2. Digital modulation maps the original data bitstreams to the IQ coordinate system according to specific mapping rules, and two branches symbols are converted into analog I and Q signals by DAC and shaping filters, respectively. It usually contains four ports, namely, analog I output, analog Q output, local oscillator (LO) port and RF input port. Many IQ modulators also support differential analog IQ inputs. The IQ demodulator includes two symmetrical branches, and each branch contains a mixer (down-conversion), and the LOs of the two mixers are homologous and orthogonal, that is, there is a 90° phase difference. After IQ demodulation, the signal processed by the low-pass filter and sampling will undergo baseband signal processing, and then the signal will be recovered.

The IQ modulator has three key performance indicators: (1) the frequency response within the entire bandwidth. (2) the symmetry of the amplitude-frequency response between the two branches. (3) the orthogonality of the two LO signals that directly affects the quality of signal modulation. The frequency response of an IQ modulator includes an amplitude-frequency response and a phase-frequency response. For an ideal linear time-invariant system, the amplitude-frequency response is flat, and the phase-frequency response is linear, respectively. And the signal can be transmitted without distortion. Therefore, the better the amplitude-frequency response and the phase-frequency response, the higher the modulation quality, and the lower the BER.

The analog IQ modulator includes mixers, which are bound to produce image frequency during the up-conversion process. Especially for the signal without frequency deviation, the center frequency of the signal is the same as the LO signal frequency of the modulator, and the image frequency product is inseparable from the signal. And it cannot be removed even if it passes through filters. Fortunately, the original IQ signal can still be adequately recovered when we adopt IQ modulators and demodulators. Due to the quadrature architecture, the IQ modulator itself has a specific image frequency rejection capability.

B. LSTM

The LSTM cell structure is shown in FIGURE 3. It turns out that they are not much different from other neural networks. LSTM has four parts, namely, forget gate layer (FGL), input gate layer (IGL), cell state and output layer, respectively, and they interact in a special way. Related equations are expressed

$$\mathbf{f}_t = \sigma(\mathbf{W}_f \cdot [\mathbf{h}_{t-1}, \mathbf{x}_t] + \mathbf{b}_f) \tag{3}$$
$$\mathbf{i}_t = \sigma(\mathbf{W}_i \cdot [\mathbf{h}_{t-1}, \mathbf{x}_t] + \mathbf{b}_i) \tag{4}$$
$$\tilde{\mathbf{C}}_t = \tanh(\mathbf{W}_C \cdot [\mathbf{h}_{t-1}, \mathbf{x}_t] + \mathbf{b}_C) \tag{5}$$
$$\mathbf{C}_t = \mathbf{f}_t * \mathbf{C}_{t-1} + \mathbf{i}_t * \tilde{\mathbf{C}}_t \tag{6}$$
$$\mathbf{O}_t = \sigma(\mathbf{W}_o \cdot [\mathbf{h}_{t-1}, \mathbf{x}_t] + \mathbf{b}_o) \tag{7}$$
$$\mathbf{h}_t = \mathbf{O}_t * \tanh(\mathbf{C}_t) \tag{8}$$

where σ denotes the sigmoid function, and it maps a real number to the interval (0,1) and can be used for dichotomy. In (3), FGL outputs a vector composed of 0 and 1. C_t is our cell state in current state and decides what we are going to output. The next is to decide what new information we are going to store in the cell state. (4) decides which values we will update, and a tanh layer creates a vector of new candidate values $\tilde{C}_t$, which will be added to the state in (5). Then, we need to update the old cell state C_{t-1} into the new state C_t. We multiply C_{t-1} by f_t to forget the things we decided to forget earlier. (6) scales each state value according to the regulations, and the output C_t is the current cell state output but will be a filtered version. (7) (8) decide what we are going to output. x_t and h_t are current input and output vectors, respectively.

For all DL networks and its integrated structures, they require offline training before online deployment, and it

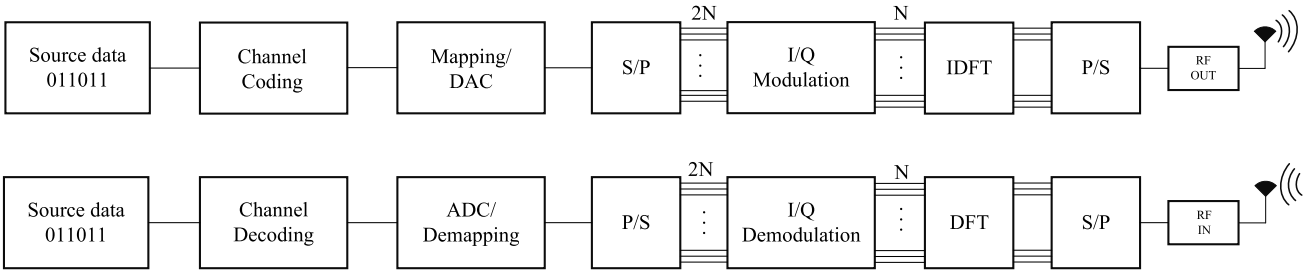

FIGURE 1. OFDM system with IQ modulation/demodulation.

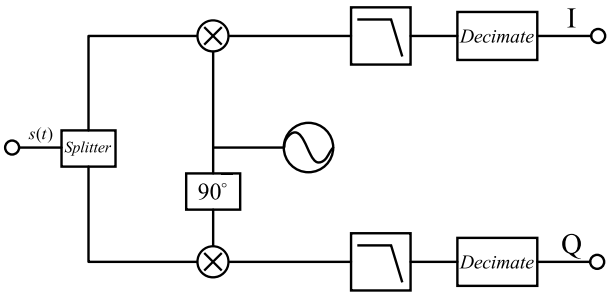

FIGURE 2. IQ demodulation.

contains forward and backward propagation process. The forward propagation process is to determine the network structure and output, and the general design adopts multi-layer LSTMs for the fitting accuracy. The back propagation process is the key to the network training, which is to determine the network parameters by comparing the forward propagation results with the real values. And the most important thing is that a large amount of labelled data is needed. In this paper, a large amount of discrete received IQ signals and the original values are selected from simulation data and labeled manually.

Algorithm 1 The Proposed DL Schemes Training Process

Input: input IQ signal in one or two braches $\mathbf{x} \in \mathbb{R}^{N\times 1}$, Initial parameters of NNs $\mathbf{S}_{int}$
Output: estimated original IQ signal $\mathbf{y}$
  for each $v \in [1, V]$ **do**
    $\hat{\mathbf{y}}^v = \mathbf{S}^v\mathbf{x}^v$
    $\mathbf{r}^v = \mathbf{y}^v - \hat{\mathbf{y}}^v$
    $loss = \frac{1}{n}\sum_{j=1}^{n}(\mathbf{r}^v)^2$
    for each $t \in [1, T]$ **do**
      $\mathbf{S}_t = \mathbf{S}_{t-1} - lr * \frac{\partial loss}{\partial \mathbf{S}_{t-1}}$
    end for
    $\tilde{\mathbf{b}^v} = \mathbf{S}_T^v\mathbf{x}^v$
  end for
  $\mathbf{y} = \tilde{\mathbf{b}^V}$
  return y

The network training pseudocode is shown in Algorithm 1, the input data is one or two branches of N sized signal x and the initial parameter of lstms $\mathbf{S}_{int}$, and the output is the

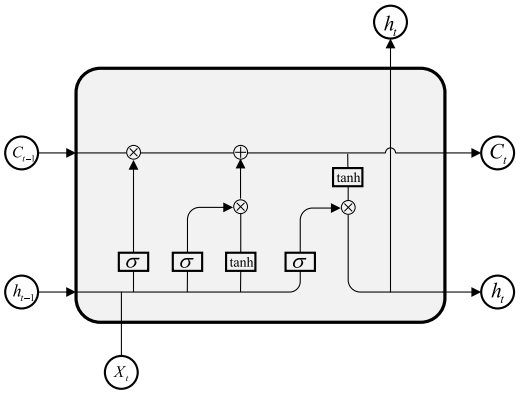

FIGURE 3. LSTM cell structure.

estimated original data $\mathbf{y}$ with n dimensions. And V is the training iterations that is carefully selected for the expected output. Taking the v-th iteration as an example, the output estimated value $\hat{\mathbf{y}}$ is the operation result of the neural network parameters and the input data, that is, the forward propagation process. Then, it exploits the MSE loss function to reversely update the parameter $\mathbf{S}^v$ after T operations based on the difference between the estimated value and the true value. Finally, we can get the esimated original signals $\mathbf{y}$.

III. IQ SYMBOLS PROCESSING SCHEMES BASED ON LSTM

In this section, the proposed DL schemes (i.e., deep learning algorithm (DLA), ensemble deep learning algorithm (EDLA), PAPR detection net (PDNet)) for signal processing are explained with simulation results, and this section is divided into three subsections. Section A is our initial design based on LSTMs. We evaluate the performance compared to the DNet proposed in [7]. By adopting LSTM networks that experts in processing sequence data, the problems and deficiencies in [7] are effectively avoided. In section B, we design a novel architecture based on digital IQ demodulation, and the design ideas derive from [12]. In that literature, the authors proposed several sub-networks for each path and then combines sub-networks together to form the ensemble algorithm. In this paper, what we process is not the received symbols of each path but the IQ demodulated symbols. Combining with LSTMs, the design constitutes the ensemble algorithm

of subsection B in this paper. Based on the scheme of subsection B, we have fully considered the peak-to-average power ratio (PAPR) problem that occurs in OFDM system [13] in subsection C. By applying the LSTMs for clipping and signal recovery to the transmitter and receiver, PAPR reduction can be effectively implemented.

A. DEEP LEARNING ALGORITHM

In [7], the authors adopted several fully connected (FC) layers to decode the received noisy signal directly. The input nodes correspond to the number of real parts and imaginary parts of two OFDM symbols. In that OFDM scheme, 64 sub-carriers and the CP length of 16 are considered, and QPSK is used as the modulation method. In this subsection, LSTMs are used to decode IQ symbols, and the structure is shown in FIGURE 4.

As is shown in the picture, the scheme in this section combines IQ demodulation with LSTMs. The former part of the design is the digital controller (DDC). For the OFDM symbols with IQ modulation and demodulation, there are N channels of parallel data, which means that there are $2N$ real symbols. $x_I[i]$ and $x_Q[i]$ denote the I and Q channel of i-th sub-carrier, where $i = 1, 2, \ldots, N$. The nodes of hidden layers are 1 and $\frac{M}{2}$, respectively, where M is the order of the modulation method. For different modulation methods, the number of bits carried by a real symbol is different. Taking 16-QAM as an example, a single branch symbol modulated by IQ carries two bits. For $\mathrm{LSTM}_n^m(m = 1, 2.$ $n = 1, 2, \ldots, 2N)$ cells, it contains two layers of LSTMs and $2N$ time steps. Performing parallel-to-serial conversion of the bits generated from the DLA scheme at all steps, we obtain the original bitstreams.

The activation function of output in LSTM is tanh and defined as follows,

$$\tanh(x) = \frac{e^x - e^{-x}}{e^x + e^{-x}} \tag{9}$$

where

$$-\infty < x < +\infty, -1 < \tanh(x) < +1 \tag{10}$$

The shape of the tanh function is similar to the sigmoid function and can be seen from the expressions and graphs. The difference lies that the peak value of the derivative function of the tanh function is 1, which is more helpful to solve the problem of vanishing gradient. Another reason for choosing the activation function of tanh is that it is necessary to find the scale factor to normalize the energy for the signal. The number of constellation points are the same in the each quadrant, and the average energy can be calculated in one quadrant. Taking the 16-QAM modulation method as an example, four points are used to calculate the average power instead of sixteen points. The normalization constants of different modulation methods are shown in the TABLE 1 [12].

In the DLA scheme, three digital modulation methods (i.e., QPSK, 16QAM, 64QAM) widely used are adopted. The discrete signal after digital IQ demodulation will be used as the training data of the DLA scheme, and the original bits as the labels. The loss function is mean square error (MSE), and the optimizer is Adam. The optimization of parameters (i.e., weights, biases) are conducted by backpropagation algorithm.

TABLE 1. Normalization constants of modulation methods.

Modulation Scheme	Normalization Constant
QPSK	$P_N = 1/\sqrt{2}$
16QAM	$P_N = 1/\sqrt{10}$
64QAM	$P_N = 1/\sqrt{42}$

TABLE 2. Training parameters.

Parameter	Value
Modulation Methods	QPSK, 16QAM, 64QAM
Path	5
Carrier Frequency	2.6GHZ
Sub-carriers	256
CP	64
Training set	600,000
Test set	400,000
Optimizer	Adam
Loss Function	MSE

The network parameters are shown in TABLE 2. By comparing the performance of different modulation methods, it verifies the robustness and stability of the design. This paper adopts representative digital modulation methods (i.e., QPSK, 16QAM, 64QAM), which are widely used today.

The BER performances of DNet [7] and DLA under different modulation methods in this section are shown in FIGURE 5. Under the QPSK modulation method, the BER drops faster than DLA, and the performance gap is up to $2dB$ when the SNR is less than $20dB$. However, due to the limitations of DNN learning ability and the vanishing gradient problem, the BER performance of DNet will not be improved further at high SNR because the short-term nature of training samples confuses the network. In addition, the fixed SNR training process limits the performance, named as leveling effect. LSTM is an excellent variant model of RNN, which inherits the characteristics of most of the RNNs, while solving the vanishing gradient problem caused by the gradual reduction of the gradient backpropagation process. LSTM is designed to deal with problems that are highly related to time series, such as encoding, decoding, etc. For the DLA model proposed in this section, the network shows a good performance whether it adopts low-order modulation (e.g., QPSK) or high-order modulation (e.g., 16QAM, 64QAM). And for the traditional MMSE detection algorithm, taking QPSK as an example, there is a performance improvement of nearly $3dB$.

B. ENSEMBLE DEEP LEARNING ALGORITHM

FIGURE 6 shows the structure diagram of IQ symbols processing based on the EDLA scheme. Enlightened by DDC ideas, we adopt two networks similar to those proposed in Section A to form an ensemble neural network

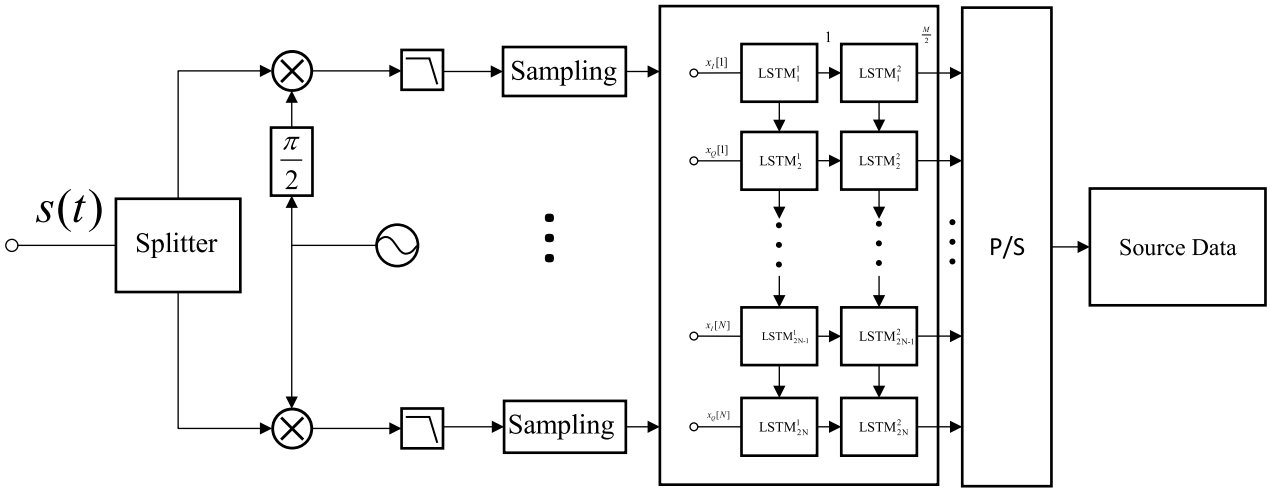

FIGURE 4. DLA scheme contains two parts: 1. The former part is the DDC technology. 2. The latter part is the signal processing with LSTMs.

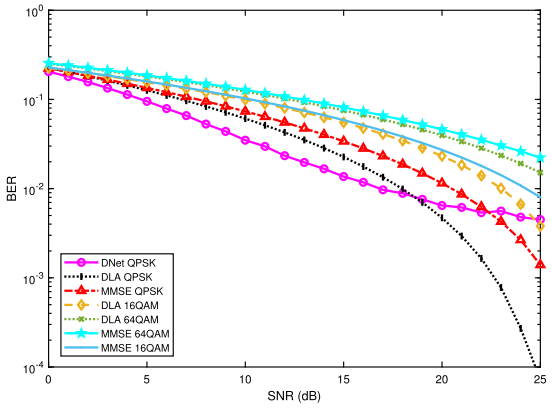

FIGURE 5. BER performance of DNet and DLA proposed in this section under different modulation methods (i.e., QPSK, 16QAM and 64QAM).

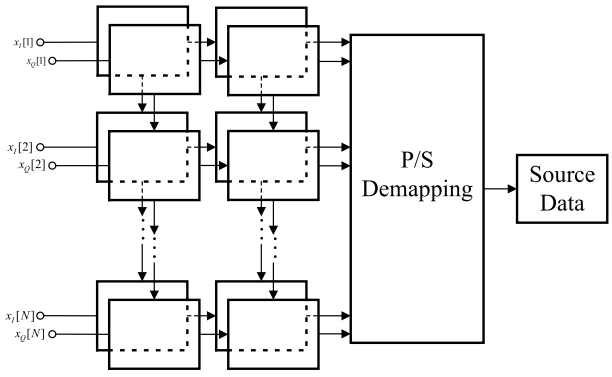

FIGURE 6. Discrete signal processing in two branches with LSTMs in EDLA scheme.

to process discrete IQ symbols. Then the symbols undergo the parallel-serial and demapping to obtain the original bitstreams.

Data-driven DL approaches heavily depends on a huge amount of labeled data nevertheless [14]. And fifth generation (5G) not only brings improvements in hardware and software [15], but also puts forward new requirements for various indicators (e.g., transmission rate, stability and packet loss rate). Combining DL with specific communication technology, the intelligence of DL helps to solve communication problems, and it also conforms to the development trend of intelligent communication. DL makes the design explainable and predictable [16], and it is constructed based on expert knowledge that developed over several decades of intense researches.

The difference between the structures shown in FIGURE 6 and FIGURE 4 lies in the way of IQ symbols processing and the form of output data. However, the performance of the scheme will be affected by the facilities, such as the orthogonality between LOs. If the orthogonality is in absence, it will bring modulation and demodulation errors (e.g., EVM and BER deterioration) when the signal without frequency deviation is generated. And the image rejection characteristic will deteriorate.

Assuming that the IQ symbols are cosine signals and orthogonal, the LO port signal is not orthogonal, and the phase difference is φ. The equations are expressed as

$$i(t) = \cos(wt); \quad q(t) = \sin(wt) \tag{11}$$

$$i_L(t) = \cos(w_c t + \varphi); \quad q_L(t) = \sin(w_c t) \tag{12}$$

$$s(t) = \frac{\sqrt{2}}{2} \cdot \sqrt{1+\cos\varphi} \cdot \cos[(w_c + w)t + \theta] + \frac{\sqrt{2}}{2} \cdot \sqrt{1-\cos\varphi} \cdot \cos[(w_c - w)t - \bar{\theta}] \tag{13}$$

In formula (11)-(13), w represents the baseband signal frequency, and w_c is the frequency of the LO ports, and φ is the phase difference of the LO ports. And the two branches of the LO port are no longer orthogonal, and the attenuation factor $\sqrt{1+\cos\varphi}$ and $\sqrt{1-\cos\varphi}$ appears in the transmitting signal. θ and $\bar{\theta}$ satisfies

$$\cos\theta = \frac{b}{\sqrt{a^2+b^2}}; \quad \cos\bar{\theta} = \frac{c}{\sqrt{c^2+b^2}} \tag{14}$$

where

$$a = \frac{1+\cos\varphi}{2}; \quad b = \frac{\sin\varphi}{2} \tag{15}$$

$$c = \frac{1-\cos\varphi}{2}; \quad b = \frac{\sin\varphi}{2} \tag{16}$$

From the formulas (11)-(16), it can be seen that the distortion of the signal and the deterioration of the system image frequency suppression performance are caused by the IQ imbalance.

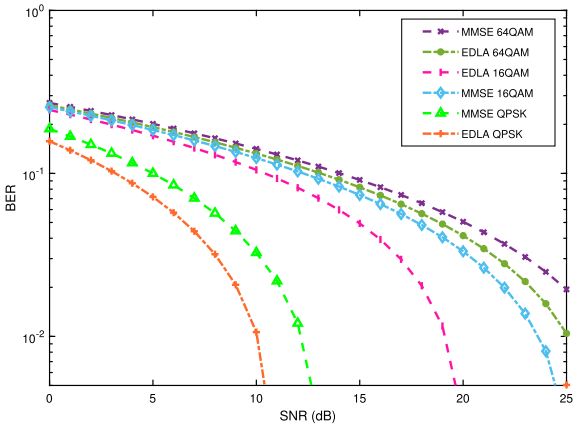

FIGURE 7. BER performance under different modulation methods.

The BER performances under different modulation methods are shown in FIGURE 7. The horizontal axis parameter is SNR, which is the ratio of the power of the output signal to the noise power output at the same time. And it is often expressed in *dB*. The training process adopts fixed SNR in the QPSK modulation scheme, so it declines at the fastest speed when SNR is 20*dB*. Moreover, QPSK only modulates the phase, and the IQ signal is easy to process, so the performance is the best. For high-order modulation (i.e., 16QAM, 64QAM), the decline is relatively slow. Compared to the DLA performance shown in FIGURE 5, there is over 2 *dB* performance improvement. FIGURE 7 mainly compares the BER performance between the proposed EDLA method and the MMSE detection algorithm. It can be seen that the performance is nearly 2dB better than the traditional algorithm. Therefore, we can improve the design performance by adjusting the network structure and depth.

Error vector magnitude (EVM) is the amplitude and phase vector difference between the ideal error-free reference signal and the actual transmitted signal at a given time. And it can comprehensively measure the amplitude and phase error of the modulated signal [17]. The formula is followed as

$$EVM = \sqrt{\frac{P_{error}}{P_{reference}}} \cdot 100\% \tag{17}$$

where P_{error} and $P_{reference}$ are the average power of the error and reference signal, respectively. According to the requirements of 5.7.1 in 3GPP TS 34.122, EVM is defined as the square root of the average power ratio of the error vector to the reference signal, and expressed as percentage. The error vector amplitude of the test UE is not more than 17.5% to avoid exceeding the target EVM requirements and increasing the transmission error of the uplinks of the channel.

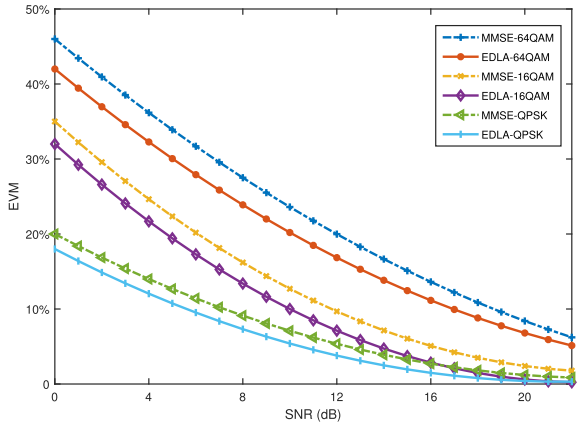

FIGURE 8. EVM performance under different modulation methods.

TABLE 3. Computational complexity of several schemes.

Parameters	Complexity
LS	$\mathcal{O}(n)$
MMSE	$\mathcal{O}(n^2)$
DLA	$\mathcal{O}(n)$
EDLA	$\mathcal{O}(2n)$
Online deployment	$\mathcal{O}(1)$

The computational complexity of different schemes is shown in Table 3. It denotes that the LS, DLA and EDLA have linear order, and the computational complexity increases linearly as input data increases. The MMSE method has the greatest complexity since it involves large-scale matrix inversion. After online deployment, the proposed schemes (i.e., DLA and EDLA) has relatively low computational complexity.

FIGURE 8 shows the EVM performance under different modulation methods. QPSK is a simple modulation method and has the lowest EVM error. For different modulation methods, its EVM under low SNR is relatively large, which shows that the scheme is greatly affected by noise. As the SNR increases, the EVM drops rapidly and approaches zero quickly at around 25*dB*. Due to the poor fitting performance of EDLA in low SNR, SNR is 2*dB*, 7*dB* and 13*dB* when EVM reach the standard of 17.5% as shown in FIGURE 8, respectively. Compared with the MMSE algorithm, the proposed method is slightly better than the traditional algorithm under different modulation methods. It shows the superiority of the design from another aspect.

C. ADAPTIVE PAPR REDUCTION NETWORK

In OFDM system, all sub-carriers after *ifft* processed will add together, so the transmitted signal has a high peak value in the time domain. Compared to single-carrier system, PAPR not only reduces the efficiency of the transmitter power amplifier, but also decreases the signal to quantization noise ratio of the analog-to-digital converter (ADC) and DAC [18]. Clipping

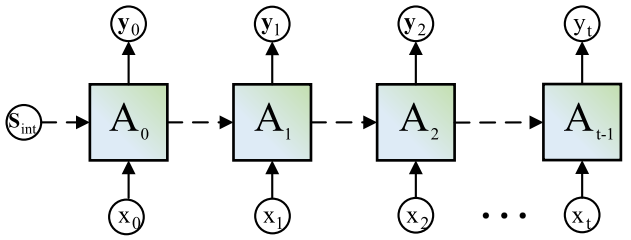

FIGURE 9. PDNet structure.

technology is the simplest method, which reduces PAPR by using limit or nonlinear saturation. It's simple to implement but may cause in-band and out-of-band interference, while also breaking the orthogonality between sub-carriers. The formula follows as

$$x_c^p[m] = \begin{cases} x^p[m], & |x^p[m]| < A \\ \dfrac{x^p[m]}{|x^p[m]|} \cdot A, & other \end{cases} \tag{18}$$

where A denotes the standard clipping level, and $x^p[m]$ represents the amplitude of the time-domain discrete signal, and $x_c^p[m]$ denotes the signal amplitude after clipping technology, respectively.

In [19], the authors proposed a PAPR reduction scheme in OFDM system based on deep autoencoder architecture, namely PRNet. It adopted DNN that is usually used for denoising corrupted symbols, and five FC layers were used for signal encoding and decoding. The PRNet reduces the probability of high PAPR by encoding the discrete frequency domain signal. In this paper, we propose a novel PAPR reduction scheme in OFDM system to clip and recover signal in the transmitter and receiver, which compromises the LSTMs based on the design of section A.

Similar to FIGURE 4, the PDNet is to clip and recover symbols in an end-to-end manner as shown in FIGURE 9. For the input data of t step, it contains t LSTM cell A and first initializes the LSTM parameters, and then propagate the data forward in order. Herein, it takes the receiver signal as input and outputs the original unclipped signal. The parameters of PDNet are shown in TABLE 4.

In TABLE 4, the number of sub-carriers N is 64, 128, 256, 512, 1024, respectively, because it is closely related to the clipping ratio (CR). CR has significant impacts on CCDF, and the expression follows as

$$CR = \frac{A}{\sigma} \tag{19}$$

where A denotes the expected magnitude and σ equals $\sqrt{N/2}$ when it is bandpass signal, and simulations are conducted to illustrate the performance of the PDNet.

CCDF defines the probability that the PAPR exceeds a certain threshold PAPR_0 in multi-carrier transmission system. FIGURE 10 shows the CCDF performance after the PDNet clips the signal under different CRs. It can be seen from the figure that as CR decreases, that is, the number of system sub-carriers increases, and the performance of CCDF decreases accordingly. The increase in N causes the

TABLE 4. Parameters of PDNet.

parameter	value
Modulation Methods	QPSK
Sub-Carriers(N)	64, 128, 256, 512, 1024
Training set	300,000
Test set	200,000
Optimizer	Adam
Loss Function	MSE

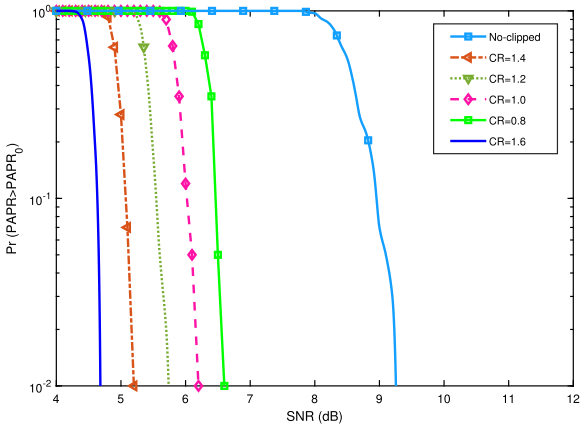

FIGURE 10. Distribution of PAPR under different CR and the performance of non-clipped.

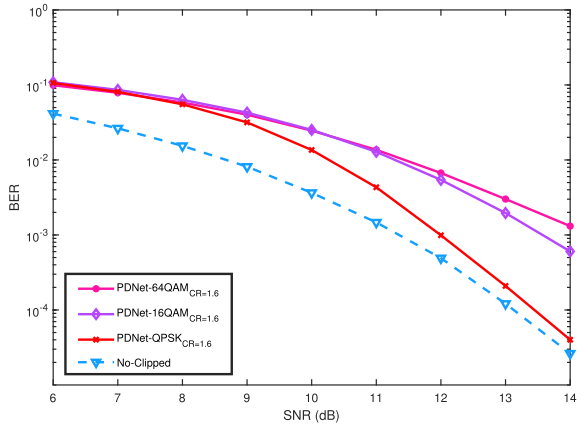

FIGURE 11. BER performance of non-clipping and clipping under different CR.

decrease in probability of high PAPR. Meantime, the high PAPR appearance probability of the signal is significantly reduced after PDNet processing compared to the one without clipping. It has least $9dB$ performance improvement in the probability of 10^{-2}.

FIGURE 11 shows the BER performance of non-clipping and clipping under different CR that is related to PAPR. Taking CR of 1.6 as an example, the signal after clipping has a $2dB$ performance loss versus the signal without clipping, which further proves that clipping operation will cause signal distortion and leads to the decrease in BER performance. It can be seen that the distortion of the signal and the deterioration of the system image frequency suppression performance are caused by the φ.

IV. CONCLUSION

In this paper, we propose three schemes (DLA, EDLA and PDNet) that implement signal processing (i.e., symbols

decoding and detection). These schemes adopt LSTMs and combine expert knowledge of digital communication with DL. The corresponding simulations are conducted to verify the effectiveness and accuracy improvements. Compared with the papers that combine DL and wireless communication currently, LSTM experts in processing sequence data and has strong adaptability. Compared with [8], though we adopt novel designs with LSTMs in time-invariant channel situation, the feasibility in the real environment needs further verification. And testing the feasibility in different channels will be our future work.

ACKNOWLEDGMENT

The sponsor was W. Zheng. I would like to express my gratitude to all those who helped me during the writing of this thesis. I gratefully acknowledge the help of supervisor, Wenjing Zheng, who has offered me valuable suggestions in the academic studies. In the preparation of the thesis, she has spent much time reading through each draft and provided me with inspiring advice. Without her patient instructions, insightful criticism and expert guidance, the completion of this thesis would not have been possible.

REFERENCES

[1] X. Li, Y. Shao, W. Fang, B. Huang, J. Zhang, S. Zou, C. Hou, and N. Chi, "Study of IQ imbalance in a single-side band radio-over-fiber system based on OFDM-MSK modulation," in *Proc. Asia Commun. Photon. Conf. Exhib.*, Dec. 2010, pp. 451–452.

[2] Y. Xu, Y. Hu, Q. Chen, and S. Zhang, "Optimal power allocation for multiuser OFDM-based cognitive heterogeneous networks," *China Commun.*, vol. 14, no. 9, pp. 52–61, Sep. 2017.

[3] T. Wang, C.-K. Wen, H. Wang, F. Gao, T. Jiang, and S. Jin, "Deep learning for wireless physical layer: Opportunities and challenges," *China Commun.*, vol. 14, no. 11, pp. 92–111, 2017.

[4] A. K. Nandi and E. E. Azzouz, "Algorithms for automatic modulation recognition of communication signals," *IEEE Trans. Commun.*, vol. 46, no. 4, pp. 431–436, Apr. 1998.

[5] E. Nachmani, Y. Be'ery, and D. Burshtein, "Learning to decode linear codes using deep learning," in *Proc. 54th Annu. Allerton Conf. Commun., Control, Comput. (Allerton)*, Sep. 2016, pp. 341–346.

[6] Y. Qiao, J. Li, B. He, W. Li, and T. Xin, "A novel signal detection scheme based on adaptive ensemble deep learning algorithm in SC-FDE systems," *IEEE Access*, vol. 8, pp. 123514–123523, 2020.

[7] H. Ye, G. Y. Li, and B.-H. Juang, "Power of deep learning for channel estimation and signal detection in OFDM systems," *IEEE Wireless Commun. Lett.*, vol. 7, no. 1, pp. 114–117, Feb. 2018.

[8] Y. Huangfu, J. Wang, R. Li, C. Xu, X. Wang, H. Zhang, and J. Wang, "Predicting the mumble of wireless channel with sequence-to-sequence models," in *Proc. IEEE 30th Annu. Int. Symp. Pers., Indoor Mobile Radio Commun. (PIMRC)*, Sep. 2019, pp. 1–7.

[9] X. Ma and Z. Gao, "Data-driven deep learning to design pilot and channel estimator for massive MIMO," *IEEE Trans. Veh. Technol.*, vol. 69, no. 5, pp. 5677–5682, May 2020.

[10] S. Liu and X. Huang, "Sparsity-aware channel estimation for mmWave massive MIMO: A deep CNN-based approach," *China Commun.*, vol. 18, no. 6, pp. 162–171, Jun. 2021.

[11] X. Ma, Z. Gao, F. Gao, and M. Di Renzo, "Model-driven deep learning based channel estimation and feedback for millimeter-wave massive hybrid MIMO systems," *IEEE J. Sel. Areas Commun.*, vol. 39, no. 8, pp. 2388–2406, Aug. 2021.

[12] C.-B. Ha and H.-K. Song, "Signal detection scheme based on adaptive ensemble deep learning model," *IEEE Access*, vol. 6, pp. 21342–21349, 2018.

[13] K. Liu, L. Wang, and Y. Liu, "A new nonlinear companding algorithm based on tangent linearization processing for PAPR reduction in OFDM systems," *China Commun.*, vol. 17, no. 8, pp. 133–146, Aug. 2020.

[14] H. He, S. Jin, C.-K. Wen, F. Gao, G. Y. Li, and Z. Xu, "Model-driven deep learning for physical layer communications," *IEEE Wireless Commun.*, vol. 26, no. 5, pp. 77–83, Oct. 2019.

[15] B. O. hAnnaidh, P. Fitzgerald, H. Berney, R. Lakshmanan, N. Coburn, S. Geary, and B. Mulvey, "Devices and sensors applicable to 5G system implementations," in *IEEE MTT-S Int. Microw. Symp. Dig.*, Aug. 2018, pp. 1–3.

[16] Z. Wang, A. Yang, P. Guo, L. Feng, and P. He, "CNN based OSNR estimation method for long haul optical fiber communication systems," in *Proc. Asia Commun. Photon. Conf. (ACP)*, Oct. 2018, pp. 1–3.

[17] J. Van lt Hof, C. De Martino, S. Malotaux, M. Squillante, M. Marchetti, L. Galatro, and M. Spirito, "Vector gain based EVM estimation at mm-wave frequencies," in *Proc. 95th ARFTG Microw. Meas. Conf. (ARFTG)*, Aug. 2020, pp. 1–5.

[18] D. S. Pawar and H. S. Badodekar, "Review of PAPR reduction techniques in wireless communication," in *Proc. IEEE Global Conf. Wireless Comput. Netw. (GCWCN)*, Nov. 2018, pp. 204–207.

[19] M. Kim, W. Lee, and D.-H. Cho, "A novel PAPR reduction scheme for OFDM system based on deep learning," *IEEE Commun. Lett.*, vol. 22, no. 3, pp. 510–513, Mar. 2018.

JUN LI received the M.S. degree in communication and information systems from Shandong University, in 2005, and the Ph.D. degree in signal and information processing from the Beijing University of Posts and Telecommunications, in 2011. He is currently a Vice Professor with the School of Electronic Information Engineering, Qilu University of Technology. His research interests include deep learning, 5G technologies, MIMO-OFDM, cooperative communication, and cognitive radio.

TONGLIANG XIN received the B.S. degree in electrical engineering from the College of Information and Business, Zhongyuan University of Technology, Zhengzhou, China, in 2018. He is currently pursuing the M.S. degree in electrical engineering and automation with the Qilu University of Technology (Shandong Academy of Sciences), Jinan, China. His research interests include wireless communication systems, signal processing, and deep learning.

BO HE received the M.S. degree in communication and information system from Shandong University, in 2002, and the Ph.D. degree in signal and information processing from the Beijing University of Posts and Communications, China, in 2006. In 2006, she joined the School of Information Science and Engineering, Shandong University. Her research interests include mobile communications and visible light communications.

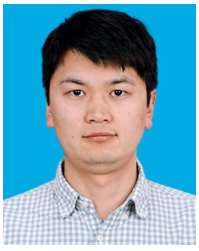

WENXIN LI received the B.S. degree in electronic and information engineering from the Qilu University of Technology (Shandong Academy of Sciences), Jinan, China, in 2019, where he is currently pursuing the M.S. degree in electrical engineering and automation. His research interests include signal processing, mobile communication systems, and deep learning.